

**IS EVIDENCE FOR RESURFACING ON VENUS BURIED DEEP WITHIN THE INTERIOR?** S. D. King<sup>1</sup> and A. C. Prunty<sup>2</sup> <sup>1</sup>Department of Geoscience, 4044 Derring Hall, Virginia Tech, Blacksburg, VA ([sdk@vt.edu](mailto:sdk@vt.edu))  
<sup>2</sup>Department of Geophysics, Colorado School of Mines, Golden, CO

**Introduction:** The surface of Venus is approximately 500-750 Myr old [e.g., 1-4]. There are two hypotheses to explain the relatively young age of the Venusian surface, progressive volcanic resurfacing or a global lithospheric overturn event [1,2,5,6]. Mantle-overturn events are controlled by a lithospheric instability whereas volcanic resurfacing events imply a plume-dominated, core-mantle boundary instability. This has significant implications for the mechanism of heat loss from the Venusian interior. The evidence consistent with catastrophic or gradual resurfacing may be buried deep within the planet.

Consider the impact of a global lithospheric instability on the deep mantle of Venus in which the entire lithosphere is subducted over a short time period. If we assume a 100-km thick lithosphere became unstable 500 Myr ago for illustration, such a resurfacing event would have placed approximately  $5 \times 10^{10} \text{ km}^3$  ( $4\pi \times 6050 \text{ km}^2 \times 100 \text{ km}$ ) of cold, dense material deep into the Venusian mantle approximately 500 Myr ago. This is approximately 5% of the volume of the planet.

A simple, back of the envelope conductive cooling calculation shows that a mass of cold, dense material from such a resurfacing event would retain a significant thermal anomaly today unless it sheared and thinned significantly as the resurfacing event unfolded. Using the analytic solution for a cooling slab after 500 Myr, at depths greater 120 km within the slab more than half the original temperature anomaly would remain [7]. While 120 km may seem like a significant fraction of the cold pile, recall that the surface area at the Venusian core-mantle boundary is one quarter that of the surface. Therefore, a 100-km thick lithosphere spread out evenly over the entire core-mantle boundary would produce a 400-km thick layer. More than likely, the anomalous cold pile would be confined to a fraction of the core-mantle boundary, hence the pile would be correspondingly thicker.

Such a cold dense pile of material would be evident in the global geoid and topography of Venus. While the geoid has no degree one term by construction, a hemispherical thermal (hence density) anomaly would be observable in the difference between the center of mass and the center of figure of the planet [8]. Yet, Venus is remarkable amongst the terrestrial planets for having the smallest offset between the center of mass and center of figure [9-10]. Thus, it is highly unlikely that a single overturn event could have been responsible for Venus' young surface age.

The geoid of Venus differs significantly from Earth and Mars in that the spectral power is not dominated by the longest wavelengths [c.f., 9]. Unlike Earth, there is a strong correlation between geoid and topography on Venus up to degrees 40 with a notably weaker correlation for degree 2 [e.g., 11]. The lack of offset between the center of mass and center of figure of Venus cannot be reconciled with the significant dense 'pile' of cold material deep in the Venusian mantle that is expected from a 'catastrophic' resurfacing event.

**Geodynamic Modeling:** We model thermal convection in a spherical shell assuming an incompressible fluid by solving conservation of mass, momentum, and energy equations using CitcomS [12]. We model the catastrophic resurfacing mechanism by implementing a temperature-dependent rheology with a lithospheric yield stress to produce stagnant-lid convection with self-generating, punctuated lithospheric instabilities. We follow the method of [13] for implementing an Arrhenius-type viscosity law and lithospheric yield stress. The temperature-dependence of the viscosity is given by

$$\eta(t) = \eta_o \exp\left(\frac{23.03}{t+1} - \frac{23.03}{2}\right), \quad (2)$$

resulting in a viscosity contrast of  $10^5$  across the domain between the non-dimensional temperatures of 0 at the surface and 1 at the core-mantle boundary. The exponential factor in the viscosity law is equal to  $\eta_o$  at  $t=1$ . The yield stress is implemented using a depth-dependent component to model brittle failure in the upper crust, and a constant ductile component to model semi-brittle, semi-ductile failure in the lower crust and lithospheric mantle

$$\eta_{yield} = \frac{\sigma_{yield}}{2\dot{\epsilon}_{II}} \quad (4)$$

where  $\dot{\epsilon}_{II}$  is the second shear strain rate invariant. The effective viscosity is then defined to be

$$\eta_{eff} = \left[ \frac{1}{\eta(T)} + \frac{1}{\eta_{yield}} \right]^{-1}. \quad (5)$$

The viscosity was then truncated between 1 and  $10^5$  for computational accuracy.

We use a Rayleigh number of  $3.5 \times 10^8$  with free-slip boundary conditions at both the surface and core-mantle boundary. The surface temperature was fixed at 725 K, and the bottom surface temperature was fixed at 3500 K. All models in this study used an initial mantle temperature of 2975 K with a 1 % tempera-

ture perturbation added at mid-mantle depth given by spherical harmonic degree  $l$  and order  $m$  in Table 1.

Model	Initial Temperature Perturbation	Ductile Yield Stress (GPa)
1	$l=1, m=0$	1, 1, -, -
2	$l=1, m=0$	*1, 1, -, -
3	$l=8, m=6$	1, 1, -, -
4	$l=1, m=0$	0.8, 0.8, -, -
5	$l=1, m=0$	4, 4, -, -
6	$l=1, m=0$	1, 1, 1, 1

Table 1. List of parameters for each model (\* indicates model includes brittle yield stress).

The time evolution of Model 1 is illustrated by the plot of the root-mean square (RMS) velocity of the entire spherical shell, the RMS surface velocity, and mobility in Fig. 1. An overturn event, indicated by the increase in surface and mantle velocities and the mobility, occurs just prior to 3 Gyr in model evolution time. For Model 2, which is identical to Model 1 with the exception of a brittle deformation layer near the surface, the mobility of the layer is a weaker even and occurs at approximately 1 Gyr. For Model 3, which is identical to Model 1 with the exception of a higher order harmonic perturbation (Table 1), the calculation remains in stagnant-lid mode with no lithospheric overturn. For Model 5, which is identical to Model 1 with the exception of a larger ductile yield stress, the model also remains in stagnant lid convection mode through out the entire model evolution. This illustrates how sensitive the overturn is to small changes in the model parameters.

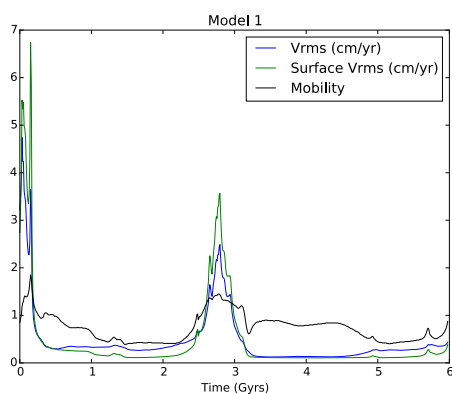


Fig. 1: RMS velocity, RMS surface velocity, and mobility for Model 1.

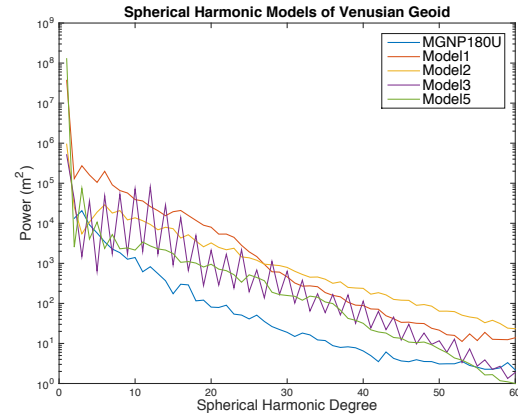


Fig. 2: Power spectra for geoid from models 1,2,3,5 compared with Venusian geoid model MGNP180U [14].

The geoid in all of the models has a large degree 2 component and greater than 1 km offset between the center of mass and center of figure (even Model 3 which begins with an  $l=8, m=6$  perturbation). The geoid spectra for all models fall off more slowly than the Venusian geoid (blue). This indicates that the lithosphere and upper mantle in our models are too weak.

The large degree 2 component of the geoid and a greater than 1 km offset between the center of mass and center of figure in our models occurs because a significant amount of cold dense material remains trapped in the lower mantle in our models, either because of the overturn event or simply as a result of the underlying degree 1 convection pattern which remains stable in the calculations that remain in the stagnant lid mode of convection. The results strongly suggest that the low degree gravity field of Venus does not support a catastrophic overturn on Venus 500 Myrs ago.

**References** [1] R. G. Strom et al. (1994) *JGR*, **99**, 10,899–10,926. [2] Herrick, R. et al. (1997), In: *Venus II* pp. 1015–1046. [3] W.B. McKinnon et al. (1997) In: *Venus II* pp. 969–1014. [4] S. A. Hauck, III et al. (1998) *JGR*, **103**, 13635–13642. [5] R. J. Phillips et al. (1991) *Science*, **252**, 651– 658. [6] D. L. Turcotte (1993) *JGR*, **98**, 17061–17068. [7] D. L. Turcotte and G. Schubert (2002), *Geodynamics*, Cambridge Press. [8] J. Wahr (1996) *Gravity and Geodesy*, Samizdat Press, pp. 293. [9] M. A. Wieczorek (2007) In: *Treatise on Geophysics*, v, 10, pp. 165– 206, Elsevier. [10] H. J. Melosh (2011) *Planetary Surface Processes*, pp.500, Cambridge. [11] M. Pauer et al. (2006) *JGR*, **111**, E11012. [12] S. Zhong et al. (2000) *JGR*, **105**, 11,063–11,082. [13] H. J. van Heck and P. J. Tackley (2008) *GRL*, **35**, L19312. [14] A. S. Konopliv et al. (1999) *Icarus*, **139**, 3–18.